Oxidation of Butane and Butene on the (100) Face of (VO)$_2$P$_2$O$_7$: A Dynamic View in Terms of the Crystallochemical Model of Active Sites

JACEK ZIÓŁKOWSKI [*,1] ELISABETH BORDES,[†] AND PIERRE COURTINE[†]

*Institute of Catalysis and Surface Chemistry, Polish Academy of Sciences, 30-239 Kraków, Poland and †Département de Génie Chimique, Université de Technologie de Compiègne, B.P. 649, 60206 Compiègne Cedex, France

The structure of the (100) face of (VO)$_2$P$_2$O$_7$ and its performance in the oxidation of n-butane and butenes to maleic anhydride have been analyzed in terms of the crystallochemical model of active sites (CMAS). Analysis involves the heats of adsorption of oxygen, hydrogen (as a component of OH), and water as well as the heats of their movement along the surface, which allows determination of the energetically easiest pathways of elementary steps and gives insight into the reaction dynamics. The catalyst (100) (VO)$_2$P$_2$O$_7$ is found to work in a surface-oxidized state, all cations being covered with oxygen. The active site for the direct oxidation of n-butane to maleic anhydride is found to be situated between four protruding, undersaturated oxygens ($2 \times$ V–O, $2 \times$ P–O). The reaction is thought to be initiated by H bonding at both terminal carbons. After removal of two terminal hydrogens, strong C$_{\text{terminal}}$–O$_{\text{surf}}$ bonds anchor the molecule sufficiently long enough for the reaction to be completed. The assemblage of unsaturated oxygens around the indicated site is geometrically and energetically convenient both for the abstraction and removal of eight hydrogens and for the insertion of three oxygens necessary for the formation of maleic anhydride. The desorption of water and migration of surface oxygen (which produces the pairs of adjacent vacancies to be filled by O$_2$ molecules) that constitute a substep of the concerted reoxidation seem to be rate determining. Oxidation of butenes on (100) (VO)$_2$P$_2$O$_7$ is thought to be initiated by adsorption of C=C over unsaturated oxygens. In view of the surface structure, this adsorption limits the number of active oxygens with which the hydrocarbon may interact and favors a mild and nonselective oxidation to epoxybutanes, crotonaldehyde, hydrofuran, furan, and acetaldehyde. Minor yields are expected due to difficult reoxidation and competitive adsorption. Theoretical predictions are shown to agree with experimental data. © 1990 Academic Press, Inc.

I. INTRODUCTION

Structure-sensitive reactions (*1, 2*) are now well known in the field of mild oxidation catalysis (*3, 4*), though the phenomenon is better called crystal face anisotropy (*5*) or catalytic anisotropy (*6*). The specificity of various crystallographic faces of a compound, with respect to the particular reactions they promote, has been most widely demonstrated for MoO$_3$ in the oxidation of propene (*3, 6–11*), methanol (*12, 13*), ethanol (*13, 14*), and allyl compounds (*5, 11*). Further examples have been reviewed (*4*), including oxidation of propene,

alcohols, and *o*-xylene on V$_2$O$_5$ (*15, 16*) and on Mn–V–Mo–O brannerite-type solid solutions (*17–19*). Catalytic anisotropy has important practical consequences. Since the more developed the "right" crystalline faces yielding the desired product, the more active and selective is the catalyst, the method of preparation can be very important. So it is in the case of V–P–O system (*20, 21*) examined further in this paper. On the other hand, when a support interacts with the active phase as in the case of V$_2$O$_5$ on TiO$_2$–anatase, the resulting coherent interfaces force the active component to expose the crystalline faces, favoring the selective oxidation of *o*-xylene into phthalic anhydride (*22–26*). In both cases, studies of

---

[1] To whom all correspondence should be addressed.

126

the external morphology of precursors, catalysts, and supports are necessary (27).

Since the crystal structure of a solid results from interactions between all the atoms, some of them being unsaturated at the surface, it is conceivable that a molecule of substrate can be "polarized" by such a surface field, which influences the way it is absorbed and the extent to which it is transformed. This is common to all solid heterogeneous catalysts. In the case of oxides (oxysalts, sulfides, etc.), the more anisotropic is the spatial distribution of atoms and metal–oxygen bond lengths, the more differentiated are the various surface fields, which legitimates the concept of catalytic anisotropy. On the basis of such presumptions a number of theoretical models (6–8, 18, 28, 29) have been proposed, including the crystallochemical model of active sites (CMAS) on oxide catalysts established by one of us (6–8).

One interesting problem on which we intend to focus our attention is the oxidation of n-butane and butenes into maleic anhydride over a V–P–O system, which apparently involves the same active phase $(VO)_2P_2O_7$ in both reactions, although the method of preparation of the catalyst greatly influences its effectiveness (20, 21). The industrial catalyst (A), highly active and selective in oxidation of n-butane (72 mol% selectivity at 98 mol% conversion) (30), is obtained by topotactic dehydration of a layered precursor which is VOH$PO_4 \cdot 0.5H_2O$ (31–37). Catalyst A is composed of $(VO)_2P_2O_7$, with the average state of (V, P) cations close to $+4.5$, and exposes predominantly the (100) face (31–33, 35). It is believed that cations V^{4+} or VO^{2+} make the active acid sites for activation of n-butane. On the contrary, the catalyst for oxidation of butenes (B) is prepared in a different way and the average oxidation state of the cations is higher; $VOPO_4$ besides $(VO)_2P_2O_7$ is detectable by X-ray diffraction, and various faces with a comparable contribution are exposed (20, 21). Oxidation of n-butane and butenes proceeds with

different kinetics: n-butane is oxidized on A directly to maleic anhydride, without noticeable formation of by-products (38, 39), whereas butenes are oxidized on B via a rake mechanism through the formation of butadiene, crotonaldehyde, and furan (40–42). While B is efficient, the activity of A in oxidation of butenes is small (43, 44). This suggests that the molecules of n-butane and butene should be adsorbed and activated in different ways. In particular, the oxidation of butene should not be a subpathway of the oxidation of n-butane; conversely, n-butane should not be oxidized through the olefin-like intermediate. Different solid-surface species or "clusters" should participate in the considered reactions.

The purpose of this paper is to discuss these problems in terms of CMAS. After the principle of the method is reviewed, the elementary steps involving adsorption and desorption, as well as movements along the surface, of oxygen, hydrogen, and water, are considered. Energetics of the hydrocarbons is briefly summarized in view of the literature data. Finally, a mechanism for the oxidation of butane and butenes on the (100) face of $(VO)_2P_2O_7$ is proposed. The theoretical results obtained are compared with experimental results from the literature under Conclusions.

2. METHOD

The crystallochemical model of active sites on oxide catalysts has been explained previously (6–8). It allows determination of the geometric and energetic maps of the surface, the nature of sites, and the most probable energy pathway of the reaction by means of calculations based on the bond length/bond strength/bond energy concept (45–47).

The geometric map of the surface is constructed by cutting the crystal along the respective crystallographic plane so as to break the weakest bonds and to conserve the stoichiometry, at least in the initial state. As a consequence some of the surface atoms gain an energy undersaturation,

conditioning active interactions with an adsorbing molecule. Undersaturated surface atoms localized in the nearest vicinity of the adsorbed molecule make an active multiplete site. Species abstracted from the molecule may move along the surface and interact with surface atoms localized in the further neighborhood. Catalytic reaction is thought to be composed of a number of elementary steps in which usually one bond is broken and another formed; however, some exo- and endothermic steps may be concerted, resulting in energy gains. The algebraic sum of the energies of the broken and formed bonds gives the net energy of the elementary step. By considering a set of consecutive steps one can construct the energy pathway of the reaction. Among a number of possible pathways the most probable is that pathway along which the endothermal barriers are the smallest. The highest of them corresponds to the rate-determining step.

As already mentioned, the energy calculations performed in terms of CMAS are based on the bond length/bond strength/bond energy concept $(45–47)$. It has been found that length R (Å), strength s (vu = valence unit), and atomization enthalpy e (kcal mol^{-1}) of the individual bond in an oxide crystal (and in some molecules) are related by the formulas

$$s = \frac{dz}{R - R_0} \qquad (1)$$

and

$$e = Js \qquad (2)$$

where z (vu) is cation valence, d (Å) and R_0 (Å) are empirical parameters (related to the ionic radii) as determined and listed in (45) for over 200 cations, and J (kcal mol^{-1} vu^{-1}) is the standard molar atomization enthalpy of a simple oxide of the considered cation per its valence unit (46). In the case of highly covalent bonds (molecules), atoms bonding to oxygen are formally treated as cations. According to (47), J factors for

various valence states (m^+, n^+) of a given cation are related by the formula

$$J_m = J_n \sqrt{n/m}. \qquad (3)$$

The energies of bonds in molecules (e.g., O–O, C–C, C–H) for which the coefficients in Eqs. (1) and (2) are not known are taken from the literature as listed in Ref. (8).

All coefficients used in this paper are gathered in Table 1. Most of them are taken from Refs. $(45, 46)$. J factor for P^{5+} was calculated using the thermochemical data from (48); J's for P^{4+} and P$^{4.5+}$ were calculated with Eq. (3) (the meaning of P$^{4.5+}$ will be explained below). Ionic radii of P^{4+} and P$^{4.5+}$ were estimated by interpolation between those of P^{5+} and P^{3+} (45) and used to determine the d and R_0 of these ions.

It seems relevant to add two remarks justifying the proposed method:

(i) For a long time $(49, 50)$ empirical relationships between bond length R and bond strength s, as well as Pauling's valence principle $\Sigma s = z$, have been used by crystallographers for such purposes as verification of determined structures, identification of atoms of different valence states that have similar X-ray scattering factors, localization of light atoms, and interpretation of the asymmetry of hydrogen bonds. The novelty of the approach offered in $(45–47)$ consists of extension of the $R–S$ relationship to bond energy. The method (CMAS)

TABLE 1

Coefficients Used in the Bond Length/Bond Strength/Bond Energy Calculations for M^{n+}–O bonds

Cation	dz (vu)	R_0 (Å)	J (kcal mol^{-1})
V^{5+}	0.3720	1.375	91.4
V^{4+}	0.3136	1.454	103.1
P^{5+}	0.4330	1.171	80.4
P$^{4.5+}$	0.4027	1.184	84.7
P^{4+}	0.3700	1.197	89.9
H^{1+}	0.1294	0.829	116.0
C^{4+}	0.4240	0.950	95.6

proposed in (6–8) and developed in (51, 52) and in the present paper is a new application of the R–s–e concept to the field of surface chemistry of solids.

(ii) Undersaturation of the surface (energy of the missing bonds) is related to surface energy. As pointed out in (52) it is advisable to distinguish between classical average surface energy E (in energy units per area) and local surface energy e (in energy units per mole of chemically and crystallographically identical atoms). E is useful for discussing various macroscopic phenomena while e, frequently exhibiting great nonhomogeneity along the surface, may serve in the consideration of the mechanisms of processes on a molecular level (e.g., CMAS). Average surface energy E_s is usually considered as the energy E_c necessary to cut the bonds in the process of surface formation lowered by the relaxation energy E_r linked with energy gains accompanying some rearrangements in the surface layer. The latter are expected to be extended solely (52, 53) or predominantly (52, 54, 55) on one outermost layer of the crystal lattice. So it is with local surface energy. As argued in (52), it is advisable to differentiate between passive surface energy (equal to E_s), which concerns static properties (e.g., equilibrium form of crystals), and active surface energy (equal or close to E_c), which is responsible for various aspects of surface reactivity and cleavage. E_r (e_r) may be considered a measure of the unexploited binding ability of the surface atoms "stored" in the intimate interatomic interactions in the top layer(s). Whole E_c (e_c) (including E_r/e_r is always ready to engage with species approaching the surface. Just active local e_c values are used in CMAS.

3. RESULTS AND DISCUSSION

3.1. Bond Lengths, Strengths, and Energies in the Bulk of $(VO)_2P_2O_7$

The structure of $(VO)_2P_2O_7$ has been determined by Gorbunova and Linde (56). It is orthorhombic, $Pca2_1$, with $a = 7.725$ Å,

$b = 16.576$ Å, $c = 9.573$ Å, and $Z = 8$. The packing of polyhedra is shown in Fig. 1. Bond lengths (56) are listed in Tables 2 and 3 along with bond strengths and energies calculated from Eqs. (1) and (2). There are four nonequivalent V atoms per unit cell localized in the distorted octahedra, four nonequivalent P atoms in the distorted tetrahedra and 18 nonequivalent oxygens. The nonequivalent atoms are indexed as, e.g., V1, P2, O5, etc; the prime (O1 and O1') is used to distinguish the two nonequivalent V1–O1 and V1–O1' bonds to oxygen of the same kind (cf. Table 2). In the structure discussed, VO_6 octahedra make pairs, edge-sharing along [010]. Each VO_6 pair, with short vanadyl bonds in the trans position, is linked by corners to the next pair, thus making the pillars along [100] infinite. The pillars are bound by isolated phosphate groups P_2O_7 composed of two PO_4-sharing corners along [100].

The strength and energy of V–O bonds (Table 2) is calculated on the assumptions that vanadium is either V^{4+} or V^{5+}. From Table 2 it is apparent that V1 and V2, on one hand, and V3 and V4, on the other, behave differently. Independently on this kind of assumption, the bond strength sums Σs around V1 and V2 are close to 4, indicating that we are dealing with V^{4+}. On the contrary, V3 and V4 treated as V^{5+} give Σs values close to 5, while when treated as V^{4+}, they give much too high bond strength sums and, in particular, irrationally high strengths of V3–O15 and V4–O13 bonds, exceeding the highest possible valence of oxygen ($s \geqslant 2$). This seems to indicate that V3 and V4 are pentavalent.

Analogous calculations have been performed for P–O bonds (Table 3), with P considered to be either P^{5+} or P^{4+}. All structurally nonequivalent P atoms behave in the same way. However, when treated as P^{5+} they give $\Sigma s \approx 4.8$, a bit too small, while when treated as P^{4+} they give $\Sigma s \approx 4.4$, which is too high. It has therefore been decided that all P atoms will be ascribed the same and intermediate valence state of 4.5.
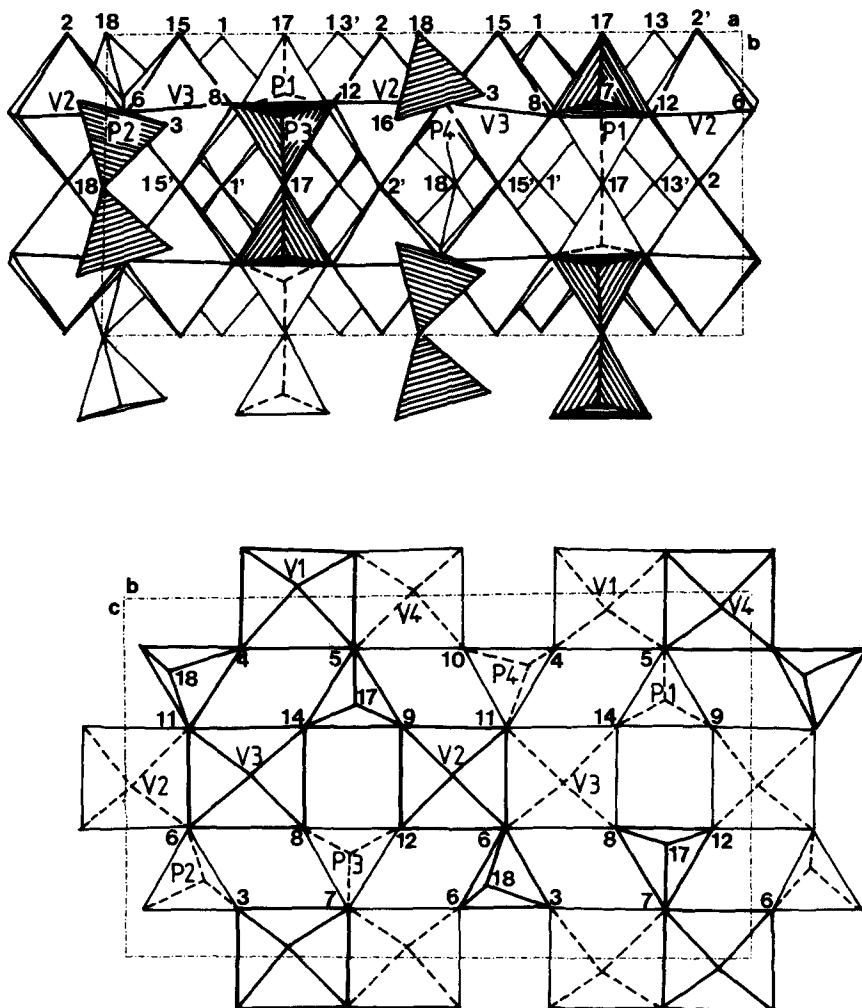
FIG. 1. Packing of the VO_6 octahedra and PO_4 tetrahedra in $(VO)_2P_2O_7$ projected on (001) and (100) planes. Nonequivalent cations are labeled V1–V4 and P1–P4; nonequivalent oxygens (O1–O18) are labeled with numbers alone. Quadrangles representing VO_6 octahedra in the (100) projection are crossed with either solid or dashed lines, which indicate the trans position of short vanadyl bonds in adjacent VO_6 groups. Analogous intersection of PO_4 triangles marks protruding and immersed corners. Further details are given in the text and in Tables 2 and 3.

Given this assumption, $\Sigma s \approx 4.6$, as may be seen in the last two columns of Table 3. Assuming the charge distribution around V and P resulting from the above considerations, we write the double formula of the compound as $V_2^{4+}V_2^{5+}P_4^{5+}O_{18}^{2-}$ which gives a balance of positive and negative charges.[2]

[2] Analogous calculations have been performed using the power-type R–s relationship $s = (R_1/R)^N$ with coefficients taken from Brown and Wu (57). Bond strength sums around all four P's are nearly the same:

5.11 ± 0.04; bond strength sums around V1, V2, V3, and V4 are 3.69, 3.79, 4.44, and 4.19, respectively (with V1–O1 and V2–O2 of about 1.15 vu and V3–O15 and V4–O13 of about 2.05 vu). This gives other valence distributions, as compared to our results, however, with much higher uncertainty. In spite of this, the trend is similar for both methods of calculation. Namely, phosphorus atoms are practically equivalent in valence while V1 and V2 differ markedly from V3 and V4. Our values for s are used in further discussion as they are more consistent and they can be transferred to the energy units [cf. Eq. (2)].

TABLE 2

Bond Length R (Å), Strength s (vu), and Energies e (kcal mol^{-1}) for V–O Bonds in (VO)$_2$P$_2$O$_7$

Bond	R	V^{4+}		V^{5+}	
		s	e	s	e
V1–O1	1.730	1.136	117.1	1.048	95.8
–O1′	2.211	0.414	42.7	0.445	40.7
–O3	1.919	0.674	69.5	0.684	62.5
–O4	1.924	0.648	68.8	0.678	61.9
–O5	2.047	0.529	54.5	0.544	50.6
–O7	2.038	0.537	55.4	0.561	51.3
		3.938		3.960	
V2–O2	1.704	1.254	129.3	1.131	103.3
–O2′	2.169	0.439	45.3	0.469	42.8
–O6	2.053	0.524	54.0	0.549	50.1
–O9	1.935	0.652	67.2	0.644	60.7
–O11	2.043	0.532	54.9	0.557	50.9
–O12	1.917	0.677	69.8	0.686	62.7
		4.078		4.036	
V3–O15	1.531	4.072?		2.385	217.9
–O15′	2.339	0.354	36.5	0.386	35.3
–O6	2.041	0.534	55.1	0.558	51.1
–O8	1.976	0.601	61.9	0.619	56.6
–O11	2.084	0.498	51.3	0.525	48.0
–O14	1.947	0.636	65.6	0.650	59.4
		6.695?		5.123	
V4–O13	1.551	3.233?		2.114	193.2
–O13′	2.367	0.346	35.6	0.377	34.5
–O5	2.090	0.493	50.8	0.520	47.6
–O7	2.067	0.512	52.7	0.538	49.1
–O10	2.001	0.573	59.1	0.594	54.3
–O16	1.961	0.619	63.8	0.635	58.0
		5.776?		4.778	

Note. Vanadium is assumed to be V^{4+} or V^{5+}. Values of s having no physical meaning (proving that the attempted assumption was false) are followed by a question mark.

The preceding assumption concerning P$^{4.5+}$ is convenient to have the charge balance but it has a minor influence on the individual s and e values of P–O bonds. Namely, independently of the kind of assumption (P^{4+}, P^{5+}, P$^{4.5+}$) the uncertainty of the individual s values is at most ±5% and the uncertainty of the individual e values is at most ±2%.

Bond strength sums around all oxygens in the structure are listed in Table 4. In most cases the Σs values are between 1.84 and 2.16 and thus fit well the valence of oxygen. This is not so, however, for O1, O2, O13, and O15 which make the asymmetrical V=O. . .V bridges in the structure. The discrepancies observed seem to indicate that the coordinates of these oxygens have not been well determined. It is expected that V1–O1 and V2–O2 bonds should be shorter while V3–O15 and V4–O13 should be longer. Nevertheless, the above reservation has a minor influence on further considerations because the V1–O1, V2–O2,

TABLE 3

Bond Length R (Å), Strength s (vu), and Energies e (kcal mol^{-1}) for P–O Bonds in $(VO)_2P_2O_7$

Bond	R	P^{5+}		P^{4+}		$P^{4.5+}$	
		s	e	s	e	s	e
P1–O5	1.566	1.096	88.1	1.003	90.1	1.054	89.3
–O9	1.489	1.362	109.5	1.267	113.9	1.320	111.8
–O14	1.520	1.241	99.8	1.146	103.0	1.199	101.5
–O17	1.569	1.088	87.5	0.995	89.4	1.046	88.6
		4.787		4.411		4.619	
P2–O3	1.482	1.392	111.9	1.298	116.7	1.352	114.4
–O6	1.559	1.116	89.7	1.022	91.9	1.074	90.9
–O16	1.520	1.241	99.8	1.146	103.0	1.199	101.5
–O18	1.577	1.067	85.7	0.974	87.5	1.025	86.8
		4.816		4.440		4.650	
P3–O7	1.568	1.091	87.7	0.997	89.7	1.047	88.8
–O8	1.514	1.262	101.5	1.167	104.3	1.220	103.4
–O12	1.482	1.392	111.9	1.298	116.7	1.351	114.5
–O17	1.561	1.110	89.3	1.016	91.4	1.068	90.5
		4.855		4.478		4.686	
P4–O4	1.475	1.424	114.5	1.331	119.7	1.384	117.2
–O10	1.523	1.230	98.9	1.135	102.0	1.188	100.5
–O11	1.558	1.119	90.0	1.025	92.1	1.077	91.2
–O18	1.582	1.054	84.7	0.961	86.4	1.012	85.7
		4.827		4.452		4.661	

Note. The valence state of P is assumed to be either P^{5+} or P^{4+} or $P^{4.5+}$.

V3–O15, and V4–O13 bonds are decidedly the strongest and the V1–O1′, V2–O2′, V3–O15′, and V4–O13′ bonds are decidedly the weakest.

3.2. Surface Structure of the (100) Face of $(VO)_2P_2O_7$, Enthalpies of Sites, and Elementary Steps for Oxygen

The structure of $(VO)_2P_2O_7$ may also be described in simplified terms as composed of two layers alternating along [100]. One of them (reduced layer) contains all cations [V1, V2, V3, V4, P1, P2, P3, P4 (half of the P's being slightly immersed and half slightly protruding)] and most of the oxygens (O3, O4, O5, O6, O7, O8, O9, O10, O11, O12, O14, and O16). The second layer (oxidized layer) contains only some oxygens: O1, O2, O13, O15, O17, O18. The layers are represented in Fig. 2 and commented in further text.

Stoichiometric (100) face should be composed of a reduced layer covered with one-half of oxygens belonging to the oxidized layer (which together make the stoichiometric layer).

Let us first consider the external reduced layer and note that all oxygens belonging to it are saturated while all cations are more or less undersaturated and may be temporarily treated as potential adsorption sites. The cation sites can be characterized by the heats of adsorption e_{ox} of the atomized oxygen which are equal to the energies of the bonds broken when such a surface is formed. For the reader's convenience the respective values of e_{ox} have been picked up from Tables 2 and 3 and gathered in Table 5 (all negative and positive heats in Tables 5–10 correspond to exothermal and endothermal reactions, respectively). Adsorption sites covered with oxygen are

TABLE 4

Bond Strength Sum Σs (vu) around Oxygens in the Bulk of $(VO)_2P_2O_7$

		V=O. . .V					
V1–O1	1.136	V2–O2	1.254	V3–O15	2.385	V4–O13	2.114
V1–O1'	0.414	V2–O2'	0.439	V3–O15'	0.386	V4–O13'	0.377
	1.550		1.693		2.771		2.491

		P—O—P					
P1–O17	1.046	P2–O18	1.025				
P3–O17	1.068	P4–O18	1.012				
	2.114		2.037				

		P—O—V					
P1–O14	1.199	P1–O9	1.320	P2–O3	1.352	P2–O16	1.199
V3–O14	0.650	V2–O9	0.652	V1–O3	0.674	V4–O16	0.635
	1.849		1.972		2.026		1.834
P3–O8	1.220	P3–O12	1.351	P4–O4	1.384	P4–O10	1.188
V3–O8	0.619	V2–O12	0.677	V1–O4	0.648	V4–O10	0.594
	1.839		2.028		2.032		1.782

$$P-O\begin{cases} V \\ V \end{cases}$$

P1–O5	1.054	P2–O6	1.074	P3–O7	1.047	P4–O11	1.077
V1–O5	0.520	V2–O6	0.524	V1–O7	0.537	V2–O11	0.532
V4–O5	0.552	V3–O6	0.558	V4–O7	0.538	V3–O11	0.525
	2.126		2.156		2.122		2.134

Note. The assumed valence states of cations are V^{4+} for V1 and V2, V^{5+} for V3 and V4, $P^{4.5+}$ for all P's.

labeled as V1O1, V1O1', V2O2, etc., or briefly V1,1, V1,1', V2,2, etc.

Considering the e_{ox} values, we conclude that the sites belonging to the oxidized layer should be occupied in order of increasing energy. Thus, on passing from reduced layer to stoichiometric layer all V1,1, V2,2, V3,15, and V4,13 sites should be occupied as well as a half of P1,17, P2,18, P3,17, and P4,18 which are practically energetically equivalent. The other half of the P-type sites should remain empty as should all V1,1', V2,2', V3,15', and V4,13' sites (as explained in the legend to Fig. 3).

Let us note, however, that in reality oxygen has the choice either to be adsorbed on the undersaturated sites of the exposed reduced layer or to be in the form of O_2 molecules, the dissociation energy of which is 119.1 kcal mol^{-1}. To point out the preference we have to calculate the heats of dissociative adsorption q_{ox} of the O_2 molecule on all adjacent pairs of sites of the reduced

TABLE 5

Energy State e_{ox} (kcal mol^{-1}) of the Surface Oxygen on Various Sites on the (100) Face of $(VO)_2P_2O_7$

Site	e	Site	e
V1,1	−117.1	V4,13'	− 34.5
V1,1'	− 42.7	V4,13	−193.2
V2,2	−129.3	P1,17	− 88.6
V2,2'	− 45.3	P2,18	− 86.8
V3,15	−217.9	P3,17	− 90.5
V3,15'	− 35.3	P4,18	− 85.7

Note. V1,1 means O1 adsorbed over V1, etc.

○ **Saturated, inactive oxygen**

◉ **Adsorbed oxygen over V**

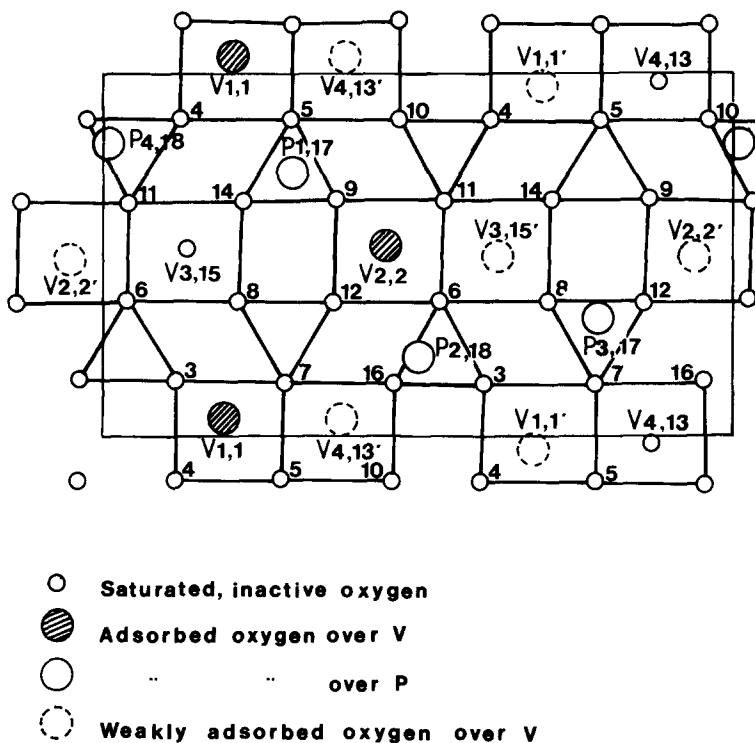◯ **"   " over P**

◌ **Weakly adsorbed oxygen over V**

FIG. 2. Structure of the oxidized (100) face of $(VO)_2P_2O_7$. V1,1 denotes oxygen O1 over V1 linked by a V1–O1 bond; so it is for all Vi,j and Pi,j atoms. Saturated inactive O3–O12, O14, and O16 (labeled in the figure with numbers alone) belong to the lower-lying reduced-layer (see text). The higher-lying oxidized layer is composed of entirely saturated V3,15, V4,13; strongly saturated ($s > 1$) V1,1, V2,2; moderately saturated ($s \approx 1$) P1,17, P2,18, P3,17, P4,18; and weakly saturated ($s \approx 0.4$) V1,1', V2,2', V3,15', V4,13'. Stoichiometric (100) face would contain in the oxidized layer all oxygens V3,15, V4,13, V1,1, V2,2 and half of P1,17, P2,18, P3,17, P4,18, the other half of P-type sites and all of $s \approx 0.4$ remaining empty.

layer. Sites less distant than 4 Å are considered adjacent. As an example, take

$$V1,\phi1 + V4,\phi13' + O_2 \rightarrow V1O1 + V4O13' \quad (4)$$
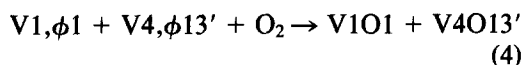
where ϕ represents the empty oxygen site. The heat of this reaction is $+119.1 - 117.1 - 34.5 = -32.5$ kcal mol^{-1}. The calculated heats for all other pairs of sites are gathered in Table 6 and the site distribution is schematically represented in Fig. 3. It is seen that all q_{ox} values are negative, which means that there is a diminution in the surface energy (52) of the (100) face when it is oxidized. Therefore in further discussion we consider the oxidized (100) face as the
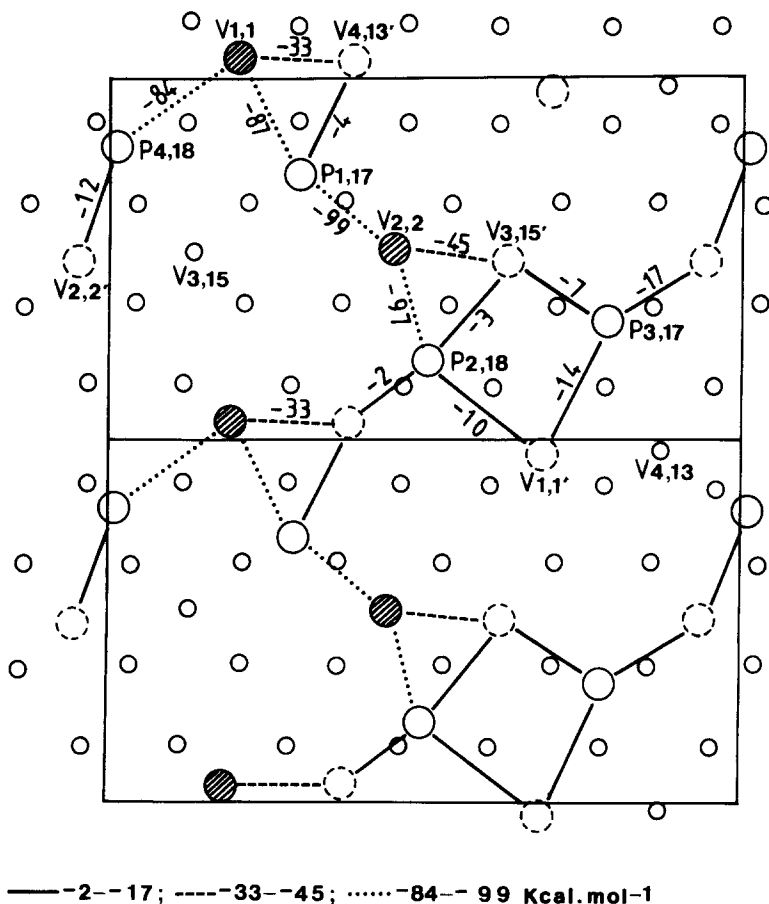
TABLE 6

Enthalpies q_{ox} (kcal mol^{-1}) of Dissociative Adsorption of O_2 on Various Pairs of the Adjacent sites on the (100) Face of $(VO)_2P_2O_7$

Site	q	Site	q
V1,1 + V4,13'	− 32.5	V2,2' + P3,17	− 16.7
V1,1 + P1,17	− 86.6	V2,2' + P4,18	− 11.9
V1,1 + P4,18	− 83.7	V3,15 + P1,17	−187.4
V1,1' + V4,13	−116.8	V3,15 + P4,18	−184.5
V1,1' + P2,18	− 10.4	V3,15 + P2,18	− 3.0
V1,1' + P3,17	− 14.1	V3,15' + P3,17	− 6.7
V2,2 + V3,15'	− 45.5	V4,13 + P3,17	−164.6
V2,2 + P1,17	− 98.8	V4,13 + P4,18	−159.8
V2,2 + P2,18	− 97.0	V4,13' + P1,17	− 4.0
V2,2' + V3,15	−144.1	V4,13' + P2,18	− 2.2

Note. V1,1 means O1 adsorbed over V1, etc.

FIG. 3. Enthalpies q_{ox} (kcal mol⁻¹) of dissociative adsorption of O_2 on various pairs of adjacent sites on the (100) face of $(VO)_2P_2O_7$. Solid, dashed, and dotted lines link the pairs of sites of different order of strength of adsorption. Background (arrangement of surface atoms) is taken from Fig. 2.

most stable one. Oxygens belonging to the oxidized (100) face of $(VO)_2P_2O_7$ and "seen" by adsorbing molecules may thus be divided into five groups: (i) entirely saturated 03–012, 014, 016 belonging to the lower-lying reduced layer; (ii) entirely saturated V3,15 and V4,13 belonging to the higher-lying oxidized layer; (iii) strongly saturated V1,1 and V2,2 ($s \approx 1.2$, $e_{ox} \approx 120$) belonging to the oxidized layer; (iv) moderately saturated P1,17, P2,18, P3,17, and P4,18 ($s \approx 1$, $e_{ox} \approx 90$) belonging to the oxidized layer; (v) weakly saturated V1,1', V2,2', V3,15', and V4,13' ($s \approx 0.4$, $e_{ox} \approx 40$) belonging to the oxidized layer. Obvi-

ously, in terms of CMAS, the sites of the (i) and (ii) groups are "dead" for catalysis. Calculated heats q_{ox} (Table 6) and e_{ox} (Table 5) will be useful further in considering the stages of catalyst reoxidation and probability of oxygen insertion into the adsorbed species, respectively.

In spite of the fact that the oxidized (100) face is energetically preferred it may happen that during the catalytic reaction an isolated oxygen vacancy is formed. Such a vacancy may be filled up as a result of movement of oxygen along the surface (and the vacancy movement in the opposite direction so as to have finally two adjacent

vacancies on which adsorption of oxygen is possible). Such movement can be described as, e.g.,

$$V1,1 + V4,\phi13' \rightarrow V1,\phi1 + V4O13'. \quad (5)$$

Using the values of e_{ox} from Table 5 we calculate the enthalpy of the process described by Eq. (5), which is $+117.1 - 34.5 = +82.6$ kcal mol^{-1}. Enthalpies of all other transfers of oxygen between surface sites q_{otr} have been calculated, gathered in Table 7, and schematically represented in Fig. 4. It is easily seen that if oxygen is to be moved through more than two sites it usually meets significant energy barriers. The latter data will be used in considering the

stages of reoxidation of catalyst according to the Mars and Van Krevelen mechanism (58). On the other hand we have to conclude that the oxidized (100) face of $(VO)_2P_2O_7$ may contain a minor number of oxygen vacancies (in positions named as group v) present as a result of the kinetic hindrance of oxygen movement along the surface.

3.3. Elementary Steps for Hydrogen and Water

During the catalytic reaction hydrogen atoms are abstracted from the adsorbed molecules; they move along the surface, combine with oxygen to form water, which
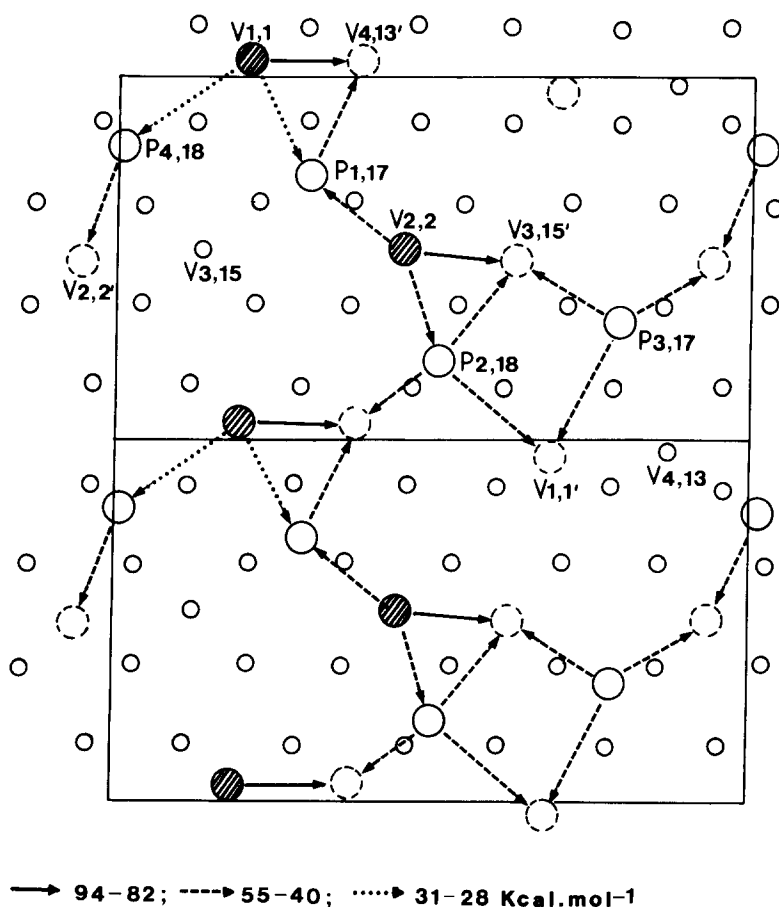

FIG. 4. Routes of movement of oxygen along the (100) face of $(VO)_2P_2O_7$. Arrows indicate endothermal steps of various heats q_{otr} (kcal mol^{-1}).

TABLE 7

Enthalpies q_{otr} (kcal mol^{-1}) of the Oxygen Transfer between Various Adjacent Sites on the (100) Face of $(VO)_2P_2O_7$[a]

Transfer (from → to)			q
V1,1	→	V4,13'	+ 82.6
V1,1	→	P1,17	+ 28.5
V1,1	→	P4,18	+ 31.4
V1,1'	→	V4,13	−150.5
V1,1'	→	P2,18	− 44.1
V1,1'	→	P3,17	− 47.8
V2,2	→	V3,15'	+ 94.0
V2,2'	→	P1,17	+ 40.7
V2,2	→	P2,18	+ 42.5
V2,2'	→	V3,15	−172.6
V2,2'	→	V4,13	−147.9
V2,2'	→	P3,17	− 45.2
V2,2'	→	P4,18	− 40.4
V3,15	→	P1,17	+129.3
V3,15	→	P4,18	+132.2
V3,15'	→	P2,18	− 51.5
V3,15'	→	P3,17	− 55.2
V4,13	→	P3,17	−102.7
V4,13'	→	P1,17	− 54.1
V4,13'	→	P2,18	− 52.3

[a] V1,1 → V4,13' means that oxygen O1, first bound to V1, is moved to V4 and becomes O13', etc. Enthalpies of transfer in the opposite direction are numerically the same but differ in sign.

is finally desorbed. Therefore, calculations analogous to those described above are done involving (i) energy states of atomized hydrogen e_h adsorbed over undersaturated surface oxygens, (ii) heats of the transfer of hydrogen q_{htr} between adjacent undersaturated surface oxygens, and (iii) heats of the evolution of water q_{wev}. The results are listed in Tables 8, 9, and 10 and the distribution of the respective sites is shown in Figs. 5 and 6.

As an example let us consider the hydrogen (first atomized) adsorbed on V1,1 and V4,13'. The strength of the V1–O1 bond is 1.136 vu and $J(V^{4+}) = 103.1$ kcal mol$^{-1} < J(H^+) = 116$ kcal mol^{-1}. According to the principle of lowest energy (8), the formation of V1–O1–H bonds, both of $s = 1$, is expected. We deal therefore with the en-

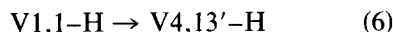TABLE 8

Energy States e_h (kcal mol^{-1}) of Hydrogen Adsorbed on Various Sites on the (100) Face of $(VO)_2P_2O_7$

Site	e	Site	e
V1,1–H	−102.0	V4,13'–H	−116.0
V1,1'–H	−116.0	P1,17–H	−112.1
V2,2–H	− 89.8	P2,18–H	−113.9
V2,2'–H	−116.0	P3,17–H	−110.2
V3,15'–H	−116.0	P4,18–H	−115.1

Note. V1,1–H means hydrogen adsorbed on O1 localized over V1, etc. No adsorption is expected over V3,15 and V4,13 as $s \approx 2$ for the V3–O15 and V4–O13 bonds.

ergy gain of -1×116 and with the energy loss of $+0.136 \times 103.1 = +14$ resulting in $e_h = -102.0$ kcal mol^{-1} for V1,1–H (Table 8). The strength of the V4–O13' bond is only 0.377; thus, the O13'–H bond of $s = 1$ is formed without a loss of energy and e_h is −116.0 kcal mol^{-1} (Table 8). It is obvious that the hydrogen transfer

$$V1,1-H \rightarrow V4,13'-H \qquad (6)$$

is linked with $q_{htr} = -14$ kcal mol^{-1} (Table 9).

Let us now assume that both sites mentioned above are occupied with hydrogen and that water H_2O13' is evolved

TABLE 9

Enthalpy q_{htr} (kcal mol^{-1}) of the Hydrogen Transfer between Various Adjacent Sites on the (100) Face of $(VO)_2P_2O_7$

Transfer (from → to)	q	Transfer (from → to)	q
V1,1–H → V4,13'–H	−14.0	V2,2–H → P2,18–H	−24.1
V1,1–H → P1,17–H	−10.1	V2,2'–H → P3,17–H	+ 5.8
V1,1–H → P4,18 –H	−13.0	V2,2'–H → P4,18–H	+ 1.0
V1,1'–H → P2,18 –H	+ 2.1	V3,15'–H → P2,18–H	+ 2.1
V1,1'–H → P3,17 –H	+ 5.8	V3,15'–H → P3,17–H	+ 5.8
V2,2–H → V3,15'–H	−26.2	V4,13'–H → P1,17–H	+ 3.9
V2,2–H → P1,17–H	−22.3	V4,13'–H → P2,18–H	+ 2.1

Note. V1,1–H → V4,13'–H means that hydrogen adsorbed on O1 over V1 is moved to O13 over V4, etc. Enthalpies of transfer in the opposite direction are numerically the same but differ in sign.
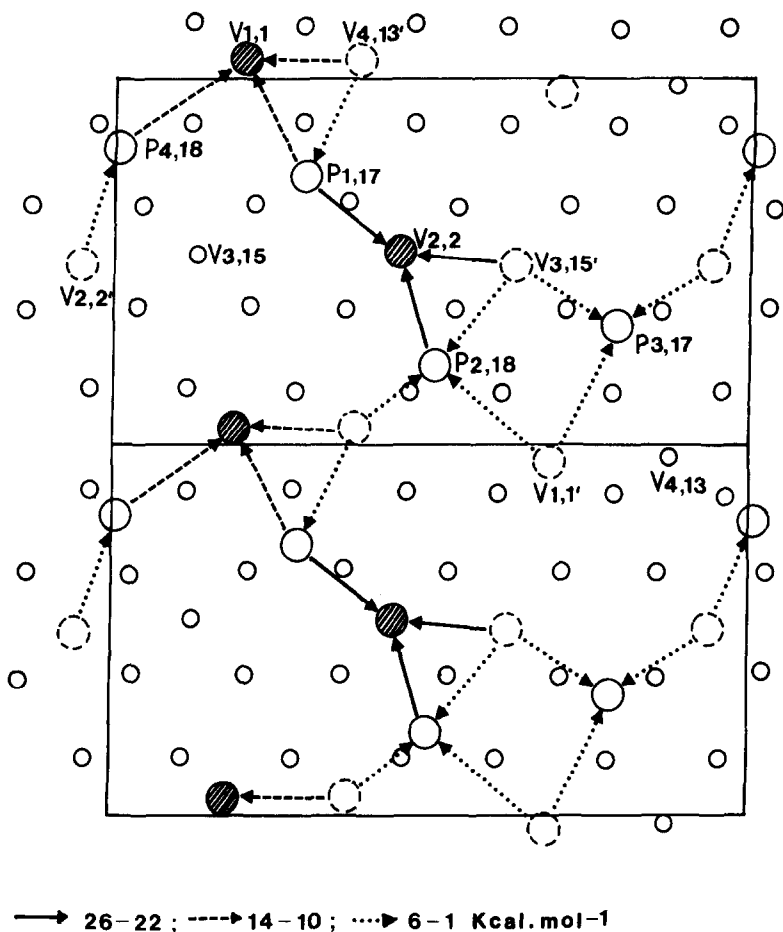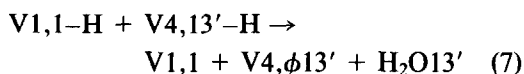
FIG. 5. Routes of movement of hydrogen along the (100) face of $(VO)_2P_2O_7$. Arrows indicate endothermal steps of various heats q_{htr} (kcal mol^{-1}).
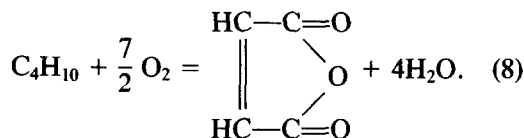
V1,1–H + V4,13′–H →

   V1,1 + V4,ϕ13′ + H$_2$O13′   (7)

In this case the V4–O13′ bond is to be broken (+34.5, cf. Table 5), hydrogen is removed from O1 and the V1–O1 bond is to be restored (+102.0), and hydrogen is removed from O1 to form O13′–H bond of $s = 1$ (−116.0 kcal mol^{-1}). The net energy of the step is thus $q_{wev} = +34.5 + 102.0 − 116.0 = 20.5$ kcal mol^{-1} (Table 10). In a similar way all effects listed in Tables 8, 9 and 10 have been calculated.

As has been pointed out (8, 45, 46), the e and s values result from the respective empirical equations and their estimated accu-

racy falls most frequently within 1–5%. To avoid inconsistencies, calculations are done with exaggerated accuracy but the final results have a meaning after reasonable rounding.

3.4. Energetics of the Molecules Taking Part in the Catalytic Process under Consideration

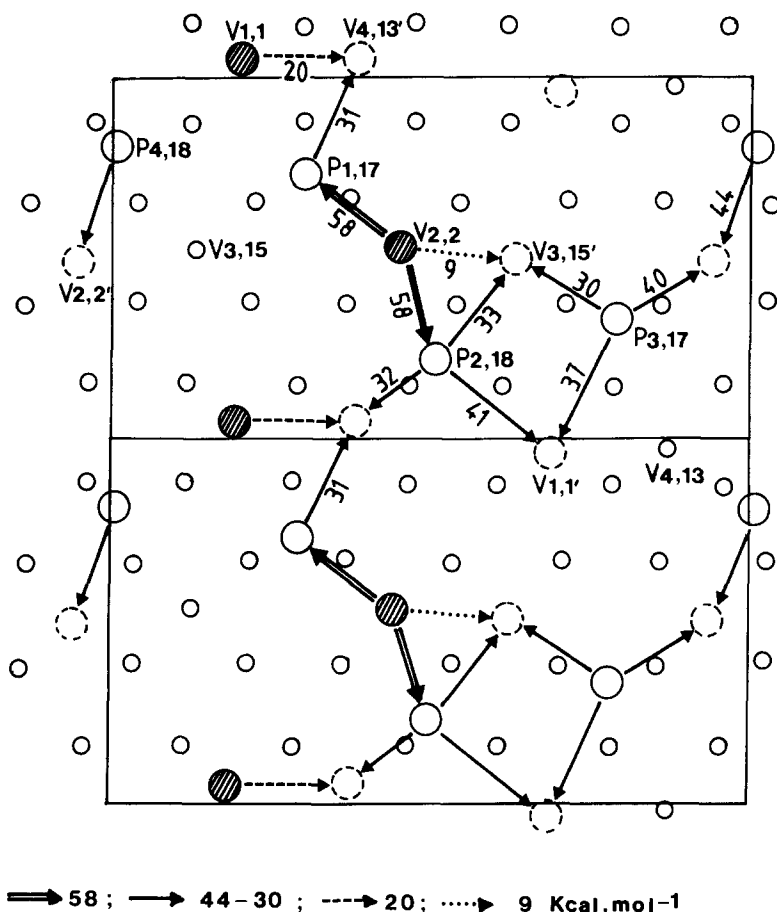The oxidation of butane considered is described by the equation

$$C_4H_{10} + \frac{7}{2}O_2 = \begin{array}{c} HC\!-\!C\!\!=\!\!O \\ \| \qquad \diagdown \\ \| \qquad \quad O \\ \| \qquad \diagup \\ HC\!-\!C\!\!=\!\!O \end{array} + 4H_2O. \quad (8)$$

FIG. 6. Enthalpies q_{wev} (kcal mol⁻¹) of evolution of water from various pairs of the adjacent sites on the (100) face of $(VO)_2P_2O_7$. Arrows indicate the direction of the transfer of hydrogen and point to the OH to be removed. All effects are endothermal.

The energy of dissociation of O_2 is 119.1 kcal mol⁻¹ and the energy of each bond in water is 116 kcal mol⁻¹ (8). As the exact energies of the individual bonds in the organic molecules are not known we make use of the average values already compiled and listed in (8). These are 99 kcal mol⁻¹ for C–H, 95.6 kcal mol⁻¹ ($s = 1$) for C–O, 157.7 kcal mol⁻¹ for C=O (typical for conjugated systems), 81 kcal mol⁻¹ for C–C, and 146 kcal mol⁻¹ for C=C (the difference between C=C and C–C is thus 65 kcal mol⁻¹).

With these assumptions, reaction (8) consists of the breakdown of eight C–H (+8 × 99 = +792) and 3.5 O–O (+3.5 × 119.1 = +416.8) bonds. On the other hand a number of bonds are formed: two C–O (−2 × 95.6 = −191.2), two C=O (−2 × 157.7 = −315.4), eight O–H (−8 × 116 = −928); and one C–C is replaced by C=C (−65). The net calculated heat of reaction is thus −292.3 kcal mol⁻¹. This value is about 18% smaller than that resulting from thermochemical tables which means that C=C, C=O, and C–O bonds are probably a bit stronger than assumed or C–H bonds are weaker. The difference (being the resultant of uncertainties in energy of 25.5 bonds) has no essential influence on the present considerations.

Under the conditions of the catalytic re-

Site	q
V1,1'–H ← P2,18–H	+40.6
V1,1'–H ← P3,17–H	+36.9
V2,2'–H ← P3,17–H	+39.5
V2,2'–H ← P4,18–H	+44.3
V3,15'–H ← V2,2–H	+ 9.1
V3,15'–H ← P2,18–H	+33.2
V3,15'–H ← P3,17–H	+29.5
V4,13'–H ← V1,1–H	+20.5
V4,13'–H ← P1,17–H	+30.6
V4,13'–H ← P2,18–H	+32.4
P1,17 –H ← V2,2–H	+58.5
P2,18'–H ← V2,2–H	+58.5

Note. V1,1'–H ← P2,18–H means that the hydrogen adsorbed on O18 over P2 is moved to the V1,1'–H site and water molecule H$_2$O1' is formed and desorbed, etc. Enthalpies q_{wev} are higher for all other possible combinations of sites including the opposite H transfer between the sites indicated in this table.
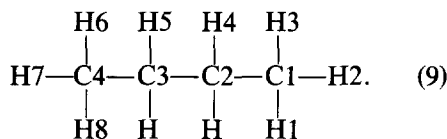
action, the molecule of butane interacts with the undersaturated surface atoms and, step by step, is transformed into the molecules of the reaction products. In the previous sections we have explained and illustrated with examples how to calculate the heats of the elementary steps in terms of CMAS. Here we would like to add one more example demonstrating how catalytic transformations of butane are initiated according to the proposed mechanism (described in detail in the next section). It is assumed that (after the molecule is fixed at the surface with H bonds) one hydrogen is abstracted from the terminal carbon (+99) and bound to the undersaturated V2,2 (−89.8, cf. Table 8 and Figs. 7, 8); simultaneously, the above-mentioned terminal carbon is bound to the surface oxygen V3,15' with a bond of $s = 1$ ($e = -95.6$ kcal mol^{-1}). The net energy of this concerted step is −86.4 kcal mol^{-1} (cf. Fig. 9, step 1).

The energy calculations for reactions of

butene are entirely analogous and are described in Section 3.6.

3.5. Proposed Mechanism of Oxidation of Butane on the (100) Face of $(VO)_2P_2O_7$

The proposed structure of the active site for the selective one-site oxidation of butane to maleic anhydride is shown in Fig. 7. Atoms of butane participating in the reaction are labeled in the following manner:

$$
\begin{array}{cccc}
\text{H6} & \text{H5} & \text{H4} & \text{H3} \\
| & | & | & | \\
\text{H7—C4—C3—C2—C1—H2.} & & & \quad(9) \\
| & | & | & | \\
\text{H8} & \text{H} & \text{H} & \text{H1}
\end{array}
$$

It is thought that first the molecule of butane is adsorbed with hydrogen bonds (e.g., C1–H1. . .O18, C4–H8. . .O2, C3–H5 . . . O17) and then undergoes the transformations according to the scheme presented in Fig. 8 with the energy effects summarized in Fig. 9.

The essential properties of the suggested active site are the following:

1. The site is located at the intersection of three routes of relatively easy movement of hydrogen along the surface (Fig. 7, routes from the molecule through oxygens C, F, and G, respectively). Therefore, hydrogens H1 and H2 may be easily transferred toward V4,13'(B) to form water H1H2O13'(B), which is desorbed (Figs. 8 and 9, steps 2, 5, 8, and 9). So it is also for H7H8O13'(A) (steps 1, 3, 4, and 12–14) and H4H5O2'(C) (steps 6, 7, 10, and 11). The easiest way for the last two hydrogens H3 and H6 is first to be transferred to P1,17–H3 and V2,2–H6, and then to wait there for reoxidation of the V3,15'(D) site and return to make water there, H3H6O15'(D) (steps 15–18, and 21–23).

2. Abstraction of the first two hydrogens (steps 1 and 2) C4H8 → V2,2(G)–H8 and C1H1 → P2,18(F)–H1 is in concert with the formation of two very strong bonds between the molecule and the catalyst, V1,1'(E)–C1 and V3,15'(D)–C4; about 197 kcal mol^{-1} is evolved in this process (Fig.
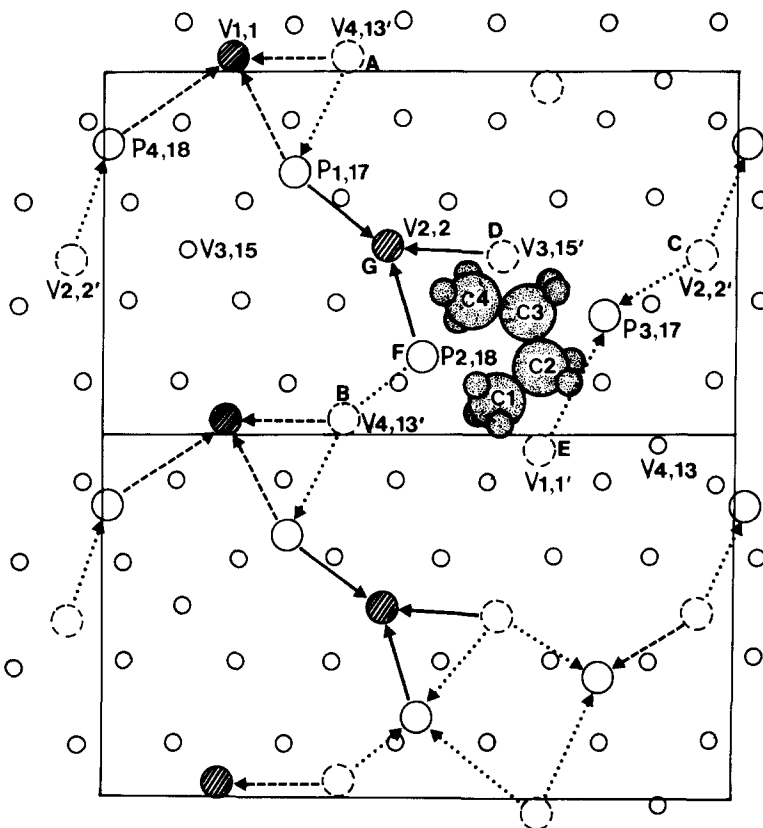
FIG. 7. Suggested structure and performance of the active site on the (100) face of (VO)₂P₂O₇ on which butane is selectively and directly oxidized to maleic anhydride. Carbons C1–C4 of the absorbed butane are labeled with numbers. Hydrogens are thought to be bound to the respective carbons as indicated in Eq. (9). For clarity of the figure and text, some oxygens are additionally labeled with letters A–G. Routes of movement of hydrogen taken from Fig. 5 provide a background. A molecule of butane is thought to be first adsorbed with H bonds between five undersaturated oxygens—P3,17, V3,15′(D), V1,1′(E), P2,18(F), V2,2(G)—on the intersection of three routes of relatively easy movement of hydrogen along the surface. Water is thought to be formed as H1H2O13′(B), H7H8O13′(A), H4H5O2′(C), and H3H6O15′(D) (the last molecule being formed after partial reoxidation of the catalyst). Oxygens V3,15′(D), V1,1′(E), and P2,18(F) are thought to be incorporated to form maleic anhydride. A detailed scheme of the reaction is shown in Fig. 8 and described in the text. Figure 9 gives the enthalpy pathway of the process.

9). With these bonds the molecule is strongly anchored to the surface long enough for the reaction to be completed. In Fig. 7 the molecule of butane has been drawn in the *cis* conformation, which is true after adsorption. But initially each conformation is good, provided that the terminal carbons attracted by the strongly undersaturated V3,15′(D) and V1,1′(E) fall in their vicinity to form first the hydrogen bonds and then to be engaged in the above-mentioned strong interactions with the surface.

3. It is important that the molecule has direct contact with five active oxygens: V2,2; P2,18; V1,1′; P3,17; and V3,15′. Three of them (V2,2; P2,18; and P3,17) make bridges through which hydrogens from all four carbon atoms may move away (as has been discussed in point 1). Two of
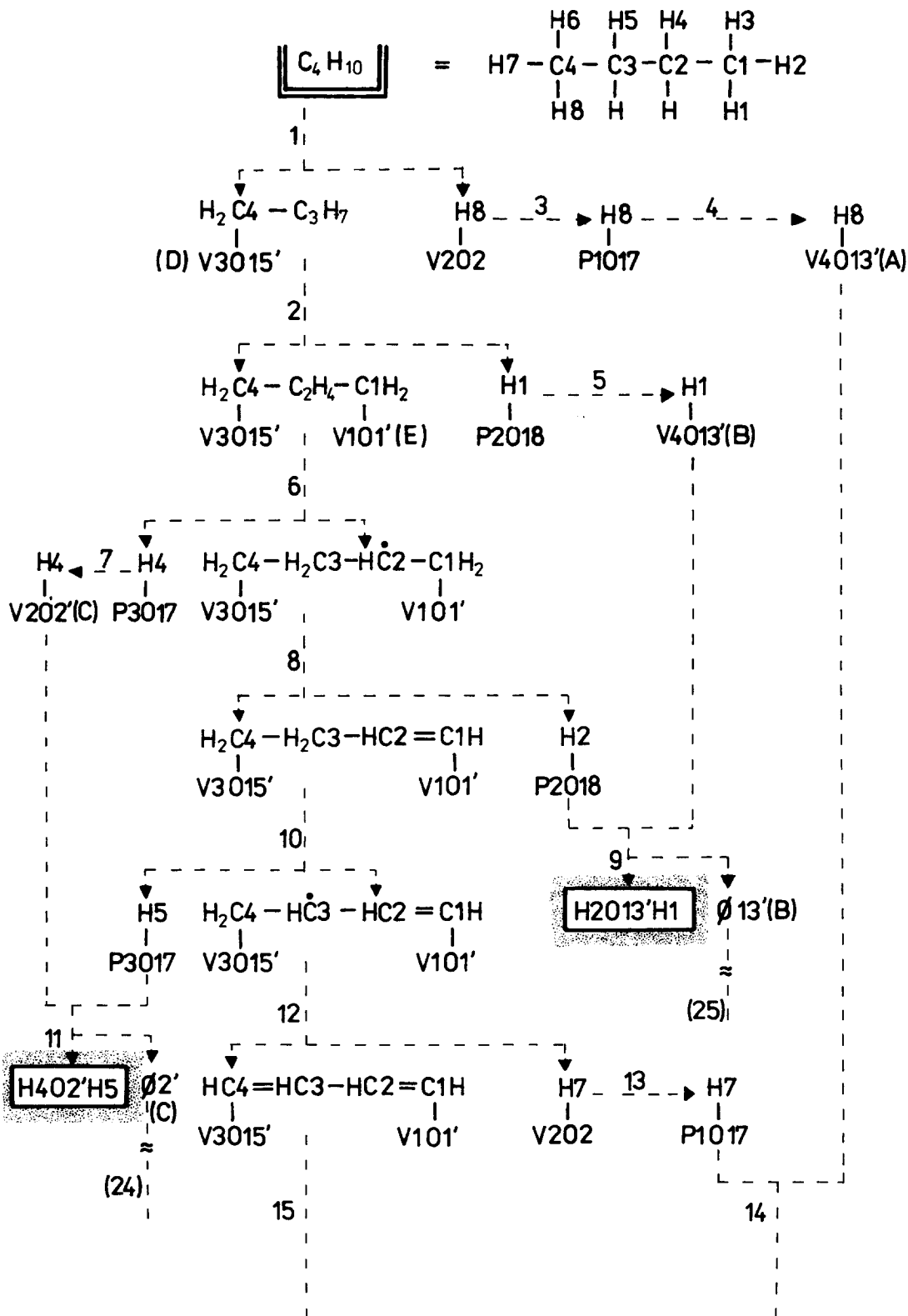
C₄H₁₀ = H7 — C4 — C3 — C2 — C1 — H2 with hydrogens H6, H5, H4, H3 on top and H8, H, H, H1 on bottom

1

H₂C4 — C₃H₇ (D) V3015'   H8 V2O2 —3→ H8 P1O17 —4→ H8 V4O13'(A)

2

H₂C4 — C₂H₄ — C1H₂ V3O15' | V1O1'(E)   H1 P2O18 —5→ H1 V4O13'(B)

6

H4 ◄ 7 — H4   H₂C4 — H₂C3 — HĊ2 — C1H₂
V2O2'(C) P3O17 V3O15'   V1O1'

8

H₂C4 — H₂C3 — HC2 = C1H V3O15'   V1O1'   H2 P2O18

9

H₂C4 — HĊ3 — HC2 = C1H   H5 P3O17 V3O15'   V1O1'   H2O13'H1   Ø13'(B)
≈
(25)

10

11

H4O2'H5   Ø2'(C)   HC4 = HC3 — HC2 = C1H V3O15'   V1O1'   H7 V2O2 —13→ H7 P1O17
≈
(24)

12

15

14

FIG. 8. Scheme of the one-site direct transformation of butane to maleic anhydride on the active site localized on the (100) face of (VO)₂P₂O₇ (cf. Figs. 7 and 9 and the text). Reaction substrates are double-framed; products are shaded.

142

15

HC4=HC3—HC2=C1
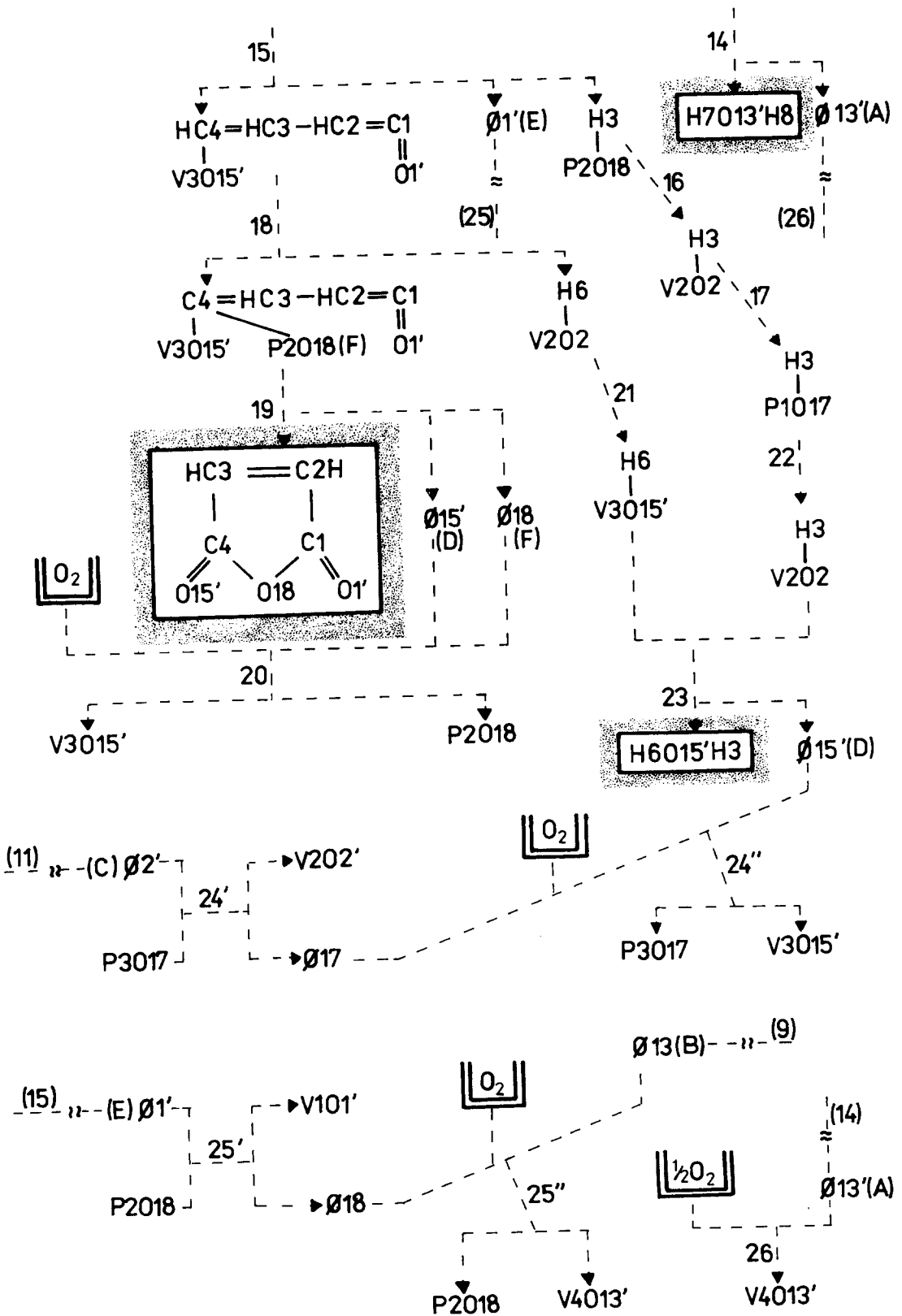V3O15'
O1'
Ø1'(E)
H3
P2O18

14

H7O13'H8
Ø13'(A)

16

H3
V2O2

(25)

(26)

18

C4=HC3—HC2=C1
V3O15' P2O18(F)
O1'

H6
V2O2

H3
V2O2 17

H3
P1O17

19

HC3 ═══ C2H

C4   C1

O15'   O18   O1'

Ø15'
(D)

Ø18
(F)

H6
V3O15' 21

22

H3
V2O2

O₂

20

V3O15'

P2O18

23

H6O15'H3

Ø15'(D)

O₂

24"

(11) ıı—(C) Ø2'

24'

→V2O2'

P3O17

→Ø17

P3O17   V3O15'

Ø13(B)— ıı—(9)

(15) ıı—(E) Ø1'

25'

→V1O1'

O₂

(14)

Ø13'(A)

P2O18

→Ø18

25"

½O₂

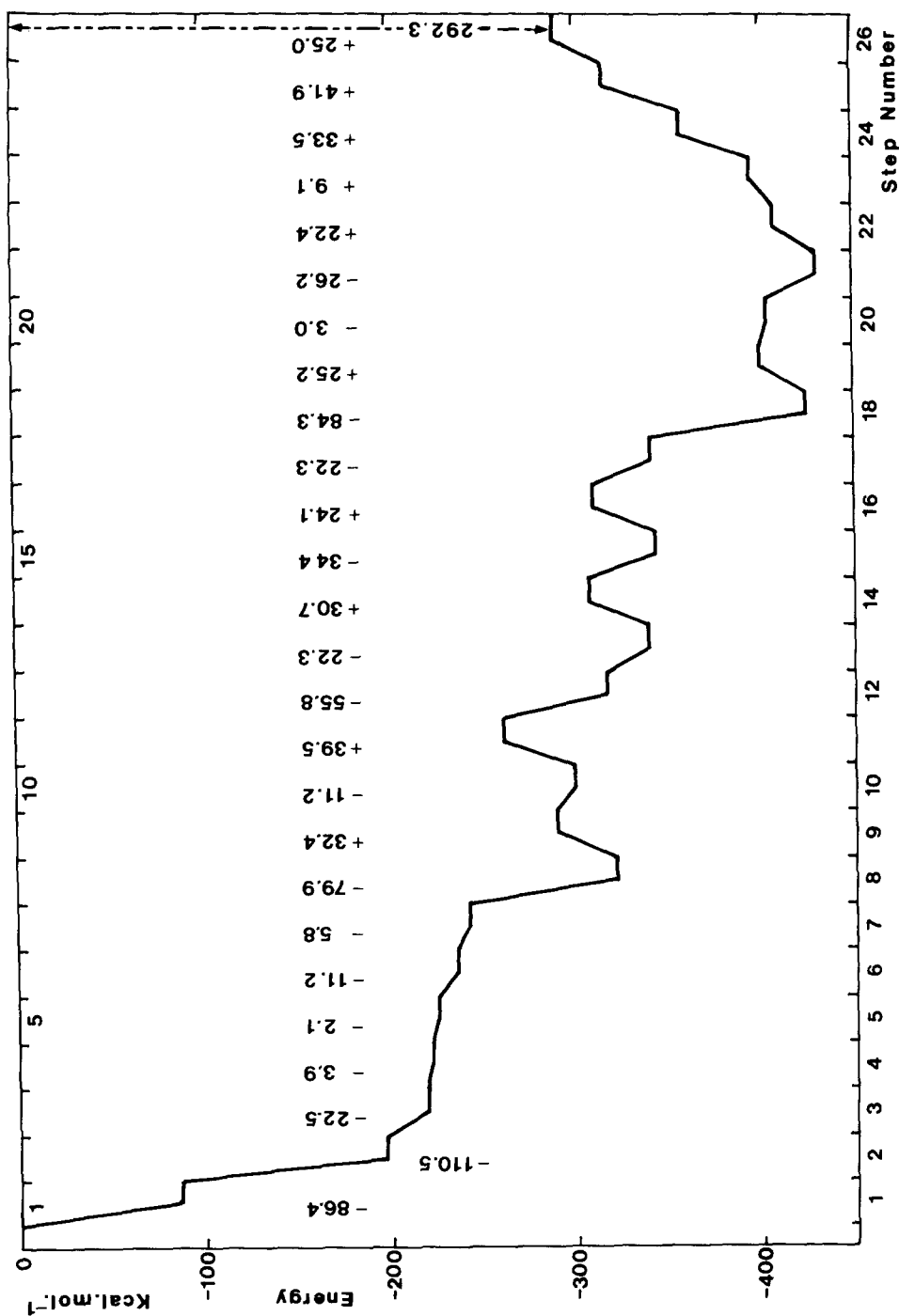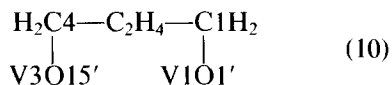P2O18   V4O13'

26

V4O13'

FIG. 8—Continued
143

FIG. 9. Energy pathway of the one-site transformation of butane to maleic anhydride on the active site localized on the (100) face of $(VO)_2P_2O_7$ (cf. Figs. 7 and 8 and the text).
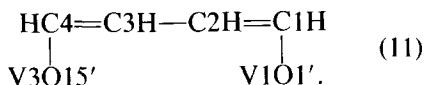
them (highly undersaturated V1,1' and V3,15') participate in the above-indicated strong anchoring of terminal carbons, and three of them (the same as before, V1,1' and V3,15', along with P2,18) are in convenient geometry to be finally incorporated into the organic species to form the molecule of maleic anhydride.

4. In particular it is important that at least two active oxygens are present in the vicinity of C4 (the same for C1) of the adsorbed butane. A bifurcated butane–surface interaction is thus possible in which the undersaturation of C4 (and C1), resulting from abstraction of the first hydrogen, is immediately compensated by the formation of a C–O_{surf} bond. As a consequence, the second hydrogen may be abstracted from each of the indicated carbons without producing a high local undersaturation on these carbons. Radicals lacking one C–H bond appear twice in the proposed mechanism (Fig. 8). The barely probable $-\ddot{C}-$ radical never appears.
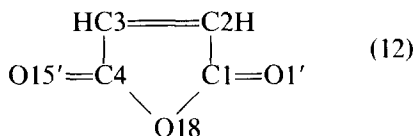
5. The main intermediate forms of butane consumed are "oxidized butane" formed in step 2

$$\begin{array}{ccc} H_2C4\!\!-\!\!C_2H_4\!\!-\!\!C1H_2 \\ | \qquad\quad | \\ V3O15' \qquad V1O1' \end{array} \qquad (10)$$

and "oxidized butadiene" formed in step 12

$$\begin{array}{ccc} HC4\!\!=\!\!C3H\!\!-\!\!C2H\!\!=\!\!C1H \\ | \qquad\qquad\quad | \\ V3O15' \qquad\qquad V1O1'. \end{array} \qquad (11)$$

Finally, in the steps 18 and 19 the ring is closed with O18(F)

$$\begin{array}{ccc} HC3\!\!=\!\!\!=\!\!\!=\!\!C2H \\ | \qquad\quad | \\ O15'\!\!=\!\!C4 \qquad C1\!\!=\!\!O1' \\ \backslash \quad\;\; / \\ O18 \end{array} \qquad (12)$$

and the molecule of maleic anhydride is ready. A butene-2-like intermediate never appears; an "oxidized butene-1-like" intermediate is formed in steps 8 and 10 but "ox-
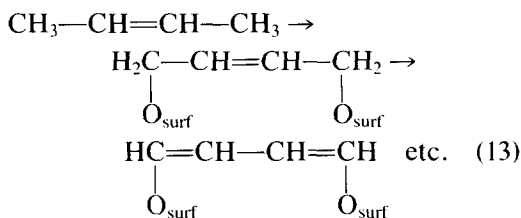
idation" occurs prior to formation of the double bond.

6. As a result of the above-mentioned processes seven oxygen vacancies are formed on the surface: V4,ϕ13'(A), V4ϕ13'(B), V2,ϕ2'(C), V3,ϕ15'(D), V1,ϕ 1'(E), P2,ϕ18(F), and, after partial reoxidation, V3,ϕ15'(D) again. The mechanism of catalyst reoxidation (Fig. 8) involves the transfer of oxygen (steps 24 and 25) which makes the highest endothermic barrier of about 40 kcal mol^{-1}. A barrier of the same height (step 11) is linked with evolution of water H4H5O2'(C). These three steps apparently determine the rate of the considered reaction.

3.6. Remarks on the Oxidation of Butenes on the (100) Face of $(VO)_2P_2O_7$

As already mentioned in the previous section, a butene-like intermediate does not appear in the mechanism proposed for the oxidation of butane and oxidation occurs prior to formation of the double bond. Thus, oxidation of butene is not a subpathway of the oxidation of butane. However, if butene was adsorbed in the way proposed for butane (H bonding followed by linkage of the terminal carbons to the surface), a reaction course (pathway 1) analogous to that shown in Fig. 8 could be initiated; e.g., for butene-2 we had

pathway 1

$$CH_3\!\!-\!\!CH\!\!=\!\!CH\!\!-\!\!CH_3 \rightarrow$$

$$\begin{array}{ccc} H_2C\!\!-\!\!CH\!\!=\!\!CH\!\!-\!\!CH_2 \rightarrow \\ | \qquad\qquad\quad | \\ O_{surf} \qquad\qquad O_{surf} \end{array}$$

$$\begin{array}{ccc} HC\!\!=\!\!CH\!\!-\!\!CH\!\!=\!\!CH \quad etc. \quad (13) \\ | \qquad\qquad\quad | \\ O_{surf} \qquad\qquad O_{surf} \end{array}$$

The main difference between the molecules of butane and butene, however, is that in the latter case the double bond exists in advance and this part of the molecule seems to be especially active in adsorption. In other words adsorption of butene through the C=C bond is thought to be
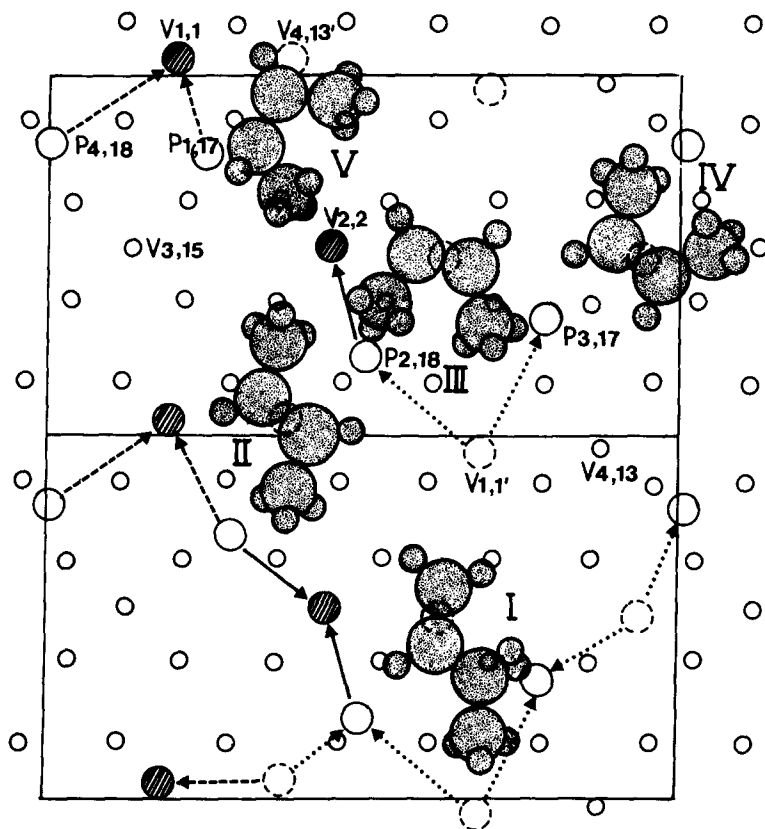
FIG. 10. Molecules of butene-1 and butene-2 adsorbed in various conformations on the (100) face of $(VO)_2P_2O_7$. Routes of movement of hydrogen taken from Fig. 5 provide a background.

strongly competitive with respect to H–bond adsorption.

As the (100) face of $(VO)_2P_2O_7$ is expected to be oxidized the most probable interaction seems to be that between the double bond of butene and the highly undersaturated surface oxygen V1,1', V2,2', V3,15', or V4,13', with formation of epoxy-type complexes which in addition may form H bonds with the adjacent surface oxygens. The heat of adsorption would be $(+65 - 150 - \Sigma e_{H bonds}$, kcal mol^{-1}, where "150" is the estimated heat of two C–O$_{surf}$–C bonds. A number of examples are shown in Fig. 10. Such adsorption should initiate the formation of epoxybutane

pathway 2

$$CH_3—CH_2—CH{=}CH_3 \rightarrow$$
$$CH_3—CH_2—CH—CH_2. \quad (14)$$
$$\underset{O}{\diagdown \diagup}$$
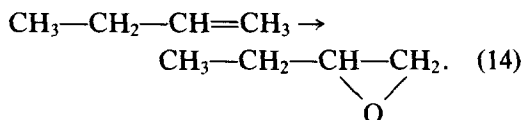
Reaction (14) may be effected in one concerted stage consisting of replacement of C=C with C–C (+65 kcal mol^{-1}), breakage of the O-lattice bond (about +40), and formation of two C=O bonds characteristic of epoxides (about −155), the net effect being about −50 kcal mol^{-1}. In view of the negative heat, this reaction should be easy (neglecting temporarily the reoxidation of the catalyst which will be discussed below).

Note that the molecule of butene ad-

sorbed in the above-indicated way (cf. Fig. 10, molecules I–IV) remains in contact usually with only one highly active oxygen belonging to group v (cf. Section 3.2), two moderately active oxygens of group iv, and sometimes, in addition, one weakly active oxygen of group iii. Taking into account the kind, number, and configuration of these oxygens, both initiation of the pathway 1 (anchoring of the terminal carbons) and insertion of the three oxygens necessary for the formation of maleic anhydride are excluded. Let us note moreover that it is very rare that two active oxygens are present in the vincinity of the same carbon, which is necessary for the bifurcate butene–surface interaction. Thus, abstraction of two hydrogens from the same carbon and formation of aldehydes or ketones are hindered. However, the bifurcate mechanism is sometimes possible. Molecule III in Fig. 10 may serve as an example; where, the left terminal carbon may interact with P2,18 and V2,2. Crotonaldehyde may be formed on this site, along with hydrofuran or furan in the case of cyclization and dehydrogenation:

pathway 3

$$CH_3-CH=CH-CH_3 \rightarrow \underset{\underset{H}{|}}{O=C}-CH=CH-CH_3 \rightarrow \cdots \qquad (15)$$
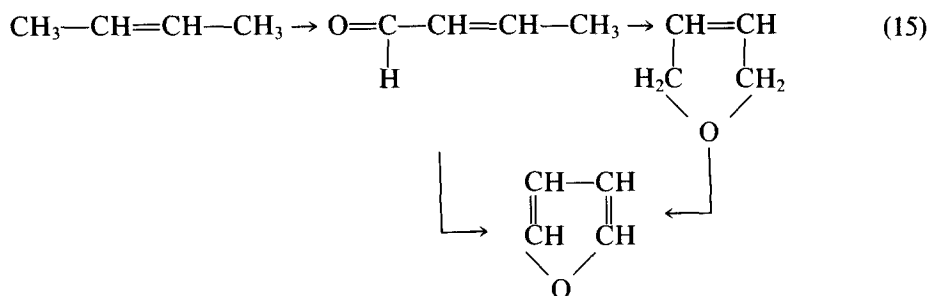
Reaction (15) seems to be easy but does not occur frequently because of the above-mentioned geometrical reasons.

It has been mentioned in Section 3.2 that in spite of the energy preference of the oxidized (100) face, some oxygens belonging to group v could be absent. In such a case butenes could form the classical π complexes over cations. The geometry of adsorption would be the same as described above for group v oxygens, pathway 2 would be excluded (in view of the absence of (group v oxygens), and pathway 3 would remain possible.

Finally let us mention that in the case of an oxidized (100) face, butene may form "peroxy"-type complexes (Fig. 10, molecule V) which could initiate pathway 4, resulting in the formation of acetaldehyde:

pathway 4

$$CH_3-CH=CH-CH_3 \rightarrow 2CH_3CHO. \qquad (16)$$
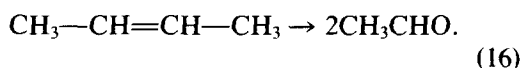
If this reaction was effected in one concerted stage comprising breakage of C=C (+146), V4–O13' (+34.5), and P1–O17 (+88.6) bonds and formation of two C=O bonds (-2×144.7, typical for aldehydes) the net effect would be about -20 kcal mol^{-1} and the process would be easy. However, independent desorption of two molecules of acetaldehyde seems more probable. The first (with O13') would be easy; the second would be linked with a significant energy barrier as a result of the necessity of breaking the P1–O17 bond. We can thus deal with the poisoning of the site by the reaction product.

The above considerations lead to the conclusion that butenes—in contrast to butane—should react on (100) $(VO)_2P_2O_7$, yielding rather slightly oxidized products consuming preferentially one (or at most two) surface oxygen per one molecule and per one site. As a result of such reactions we have to expect the formation of isolated, distant oxygen vacancies. Reoxidation of the catalyst would require long-range movement of oxygen along the surface so as to have two adjacent vacancies able to bind O_2 molecules. This process should be difficult due to both the height and the number of the energy barriers (frequency factor) met by oxygen moving along the surface. On the other hand the above-mentioned vacancies make sites for the competitive adsorption of O_2 and butene (this is not the case for butane). Adsorption of butene should thus hinder the reoxidation.

In conclusion, we have to expect (i) mild and nonselective oxidation of butenes on (100) $(VO)_2P_2O_7$ to such products as epoxybutanes, crotonaldehyde, hydrofuran, furan, and acetaldehyde, which result mainly from the geometry of adsorption; and (ii) small yields of these products due to difficult reoxidation, resulting from important barriers for movement of oxygen along the surface, competitive adsorption of substrates, and strong adsorption of some products self-poisoning the surface.

4. CONCLUSIONS

The oxidation of butane and butene on the (100) face of $(VO)_2P_2O_7$ has been considered in terms of the crystallochemical model of active sites, and mechanisms have been proposed for these reactions. Although the mechanisms are wholly in accordance with the experiments found in the literature, some additional points need to be made.

1. The surface of (100) $(VO)_2P_2O_7$ is considered predominantly oxidized in view of the calculated heats of adsorption of oxygen which are negative. This means that the coordination polyhedra of vanadium

and phosphorus are terminated by surface oxygen and/or hydroxyls, which does not contradict the fact that the average state of (V, P) cations close to 4.5+ is found in the selective catalysts by chemical analysis of the bulk of $(VO)_2P_2O_7$ (30, 36, 37, 39, 59–64). The work by Pepera et al. (39) showing that the activity of the catalyst, the surface of which is initially oxidized, drastically decreases with the number of pulses of n-butane, is in agreement with the idea of surface-oxidized (100) $(VO)_2P_2O_7$. On the other hand, such a surface resembles that of (010) γ-$VOPO_4$, which is the fully oxidized form obtained by oxidation of layered $(VO)_2P_2O_7$ coming from topotactic dehydration of $VOHPO_4 \cdot 0.5H_2O$, and which was assumed to be present as local microdomains at the steady state (19, 20, 32, 33).

2. Because it is necessary to take into account the one-step oxidation, the adsorption of n-butane is thought to be initiated by H bonding of both terminal carbons, followed (after removal of two terminal hydrogens) by a strong anchoring on the surface by means of $C_{terminal}$–O_{surf} bonds, for a time long enough to complete the reaction. This view remains in accord with the strong irreversible adsorption of butane experimentally observed (39, 65). The assemblage of undersaturated oxygens around the indicated adsorption site (including three pathways of easy movement of hydrogen along the surface) is geometrically and energetically convenient for both abstraction and removal of eight hydrogens and for the insertion of three oxygens necessary for the formation of maleic anhydride to be formed.

3. Interestingly, the surface of the V–P–O catalyst has been found (39, 66) to be rich in mobile hydroxyls, while desorption of water is difficult, even at elevated temperatures. Our calculations show that the transfer of hydrogen along the surface indeed requires an activation energy (1–26 kcal mol^{-1}, Table 9) smaller than that for desorption of water (usually 20–60 kcal mol^{-1}, Table 10). In agreement with Fig. 9 this suggests that desorption of water could be rate

determining beside the movement of oxygen along the surface, which is a substep of concerted reoxidation. The latter process is also highly activated (cf. Table 7).

4. The preceding conclusions disagree with those of others (*39, 66*), who stress that (i) reoxidation is easy, and (ii) abstraction of the first hydrogen of C2 seems to be rate determining in view of the results of H–D isotopic exchange. However, the studies on reoxidation were performed on a catalyst the surface of which was first stripped of oxygen by reduction with hydrocarbon. According to our calculations, adsorption of oxygen on such a surface (labeled "reduced layer," cf. Section 3.2) should be exothermic and therefore easy (Table 6), since O$_2$ finds adjacent vacancies to be absorbed dissociatively over cations. This is not the case at steady state when the surface is only partly reduced and oxygen vacancies are not adjacent but isolated. Movement of atomic oxygen along the surface, so as to have two neighboring vacancies, becomes the main energy barrier.

On the other hand, according to our results, the molecule of *n*-butane should be adsorbed in *cis* conformation through the terminal carbons; it may hesitate between vertical and horizontal situations with respect to the surface. If it was vertical, access to the hydrogens of C2 and C3 would be limited and therefore isotopic exchange would be hindered owing to this conformation.

5. It results from the proposed structure and performance of the active sites for *n*-butane that *essentially a (100) surface "cluster" (including the space for moving O and H species) of a size comparable to one surface unit cell should be sufficient to transform one molecule of butane into products.* These clusters could be as well ordered to form (VO)$_2$P$_2$O$_7$ detectable by X-ray diffraction, as disordered one with respect to another to form microdomains. These microdomains could be linked by means of supplementary phosphate groups which are present when P/V > 1.0. These ideas account for the "amorphous" state

and the necessity to add more phosphorous already noted by many workers using industrial selective catalysts.

6. Oxidation of butene by (VO)$_2$P$_2$O$_7$ is thought to be initiated mainly by the adsorption of C=C on undersaturated oxygens, which limits the number of active oxygens with which the adsorbed butene may interact. The expected products of this nonselective oxidation (epoxybutanes, crotonaldehyde, dihydrofuran, furan, acetaldehyde) are formed in small yields due to the difficult reoxidation and competitive adsorption. The necessity for the presence of oxidized-phase VOPO$_4$ to obtain good yields of maleic anhydride accounts for the nonactivity of the surface of (VO)$_2$P$_2$O$_7$ noted in the literature and also for the multiplicity of by-products found in the oxidation of butene.

Further applications of the CMAS concept in the V–P–O system are possible. Calculations for other planes of (VO)$_2$P$_2$O$_7$ should reinforce the specificity of the (100) face in the selective oxidation of butane and therefore account for the necessity for a careful preparation leading to an improved texture; the same approach should be taken in the oxidation of butene with VOPO$_4$.

REFERENCES

1. Boudart, M., *in* "Advances in Catalysis" (D. D. Eley, H. Pines, and P. B. Weisz, Eds.), Vol. 20, p. 153. Academic Press, New York, 1969.
2. Boudart, M., *in* "Proceedings, 6th International Congress on Catalysis, London, 1976" (G. C. Bond, P. B. Welles, and F. C. Tomkins, Eds.), Vol. 1, p. 1. Chem. Soc., London, 1977.
3. Volta, J. C., Forissier, M., Théobald, F., and Pham, T. P., *Faraday Disc. Chem. Soc.* **72,** 225 (1981).
4. Volta, J. C., and Portefaix, J. L., *Appl. Catal.* **18,** 1 (1985) and papes quoted therein.
5. Oyama, S. T., *Bull. Chem. Soc. Japan* **61,** 2585 (1988).
6. Ziółkowski, J., *J. Catal.* **80,** 263 (1983).
7. Ziółkowski, J., *J. Catal.* **84,** 317 (1983).
8. Ziółkowski, J., *J. Catal.* **100,** 45 (1986).
9. Volta, J. C., and Tatibouët, J. M., *J. Catal.* **93,** 467 (1985).
10. Ziółkowski, J., *J. Catal.*
11. Brückman, K., Grabowski, R., Haber, J., Mazurkiewicz, A., Słoczyński, J., and Wiltowski T., *J. Catal.* **104,** 71 (1987).

12. Tatibouët, J. M., and Germain, J. E., *J. Catal.* **72**, 375 (1981).
13. Tatibouët, J. M., Germain, J. E., and Volta, J. C., *J. Catal.* **82**, 240 (1983).
14. Tatibouët, J. M., and Germain, J. E., *J. Chem. Res.* (S), 286 (1981); *J. Chem. Res.* (M), 3070 (1981).
15. Tatibouët, J. M., and Germain, J. E., *C. R. Acad. Sci. Paris C* **296**, 613 (1983).
16. Gąsior, M., and Machej, T., *J. Catal.* **83**, 472 (1983).
17. Ziółkowski, J., and Janas, J., *J. Catal.* **81**, 298 (1983).
18. Ziółkowski, J., *J. Catal.* **81**, 311 (1983).
19. Ziółkowski, J., and Gąsior, M., *J. Catal.* **84**, 74 (1983).
20. Bordes, E., *Catal. Today* **1**, 499 (1987).
21. Bordes, E., *Catal. Today* **3**, 163 (1988).
22. Véjux, A., and Courtine, P., *J. Solid State Chem.* **23**, 93 (1978).
23. Véjux, A., and Courtine, P., *J. Solid State Chem.* **63**, 179 (1986).
24. Véjux, A., Bordes, E., and Courtine, P., in "Proceedings, 9th European Chemistry of Interfaces Conference, Zakopane, Poland, 1986." *Mater. Sci. Forum* **25/26**, 475 (1988).
25. Murakami, Y., Ionomata, M., Mori, K., Ui, T., Suzuki, K., Miyamoto, A., and Hatori, T., in "Preparation of Catalysts III" (G. Poncelet, P. Grange, and P. A. Jacobs, Eds.), p. 531. Elsevier, Amsterdam, 1983.
26. Gąsior, M., Gąsior, I., and Grzybowska, B., *Appl. Catal.* **10**, 87 (1984).
27. Courtine, P., *Amer. Chem. Soc. Symp. Ser.* **279**, 37 (1985).
28. Andersson, A., *J. Solid State Chem.* **42**, 263 (1982).
29. Allison, J. N., and Goddard, W. A., *J. Catal.* **92**, 127 (1985).
30. Exxon Res. Eng. Co., Yang, T. C., Rao, K. K., and Der Huang, I., U.S. Patent 4.392.986 (1987).
31. Bordes, E., Johnson, J. W., and Courtine, P., *J. Solid State Chem.* **55**, 270 (1984).
32. Bordes, E., Johnson J. W., Raminosona, A., and Courtine, P., *Mater. Sci. Monogr. B* **28**, 887 (1985).
33. Bordes, E., and Courtine, *P., J. Chem. Soc. Chem. Commun.*, 294 (1985).
34. Leonowicz, M. E., Johnson, J. W., Brody, J. F., Shannon, H. F., Jr., and Newsam, J. M., *J. Solid State Chem.* **56**, 370 (1985).
35. Cavani, F., Centi, G., and Trifiro, F., *J. Chem. Soc. Chem. Commun.*, 992 (1985).
36. Contractor, R. M., Bergna, H. E., Horowitz, H. S., Blackstone, C. M., Malone, B., Torardi C. C., Griffiths, B., Chowdhry, U., and Sleight A. W., *Catal. Today* **1**, 49 (1987).
37. David, M., Thesis, Institut de Catalyse, Lyon, France, 1988.
38. Escardino, A., Sola, C., and Ruiz, F., *An. Quim.* **74**, 1573 (1978).
39. Pepera, M. A., Callahan, J. L., Desmond, M. J., Milberger, E. C., Blum, P. R., and Bremer, N. J., *J. Amer. Chem. Soc.* **107**, 4883 (1985).
40. Ai, M., and Suzuki, S., *Bull. Chem. Soc. Japan* **47**, 3074 (1974).
41. Varma, R. L., and Saraf, D. N., *Ind. Eng. Chem. Prod. Res. Dev.* **18**, 7 (1979).
42. Cavani, F., Centi, G., Manenti, I., Riva, A., and Trifiro, F., *Ind. Eng. Chem. Prod. Res. Dev.* **22**, 570 (1983).
43. Centi, G., Manenti, I., Riva A., and Trifiro, F., *Appl. Catal.* **9**, 177 (1984).
44. Centi, G., Fornasari, G., and Trifiro, F., *J. Catal.* **89**, 44 (1984).
45. Ziółkowski, J., *J. Solid State Chem.* **57**, 269 (1985).
46. Ziółkowski, J., and Dziembaj, L., *J. Solid State Chem.* **57**, 291 (1985).
47. Ziółkowski, J., *J. Solid State Chem.* **61**, 343 (1986).
48. Kubaschewski, O., Evans, E. L., and Alcock, C. B., "Metallurgical Thermochemistry." Pergamon, Oxford/Elmsford, NY 1974.
49. Brown, I. D., in "Structures and Bonding in Crystals" (M. O'Keeffe and A. Navrotsky, Eds.), Vol. II, p. 1. Academic Press, New York, 1981, and papers quoted therein.
50. Brown, I. D., *Phys. Chem. Miner.* **15**, 30 (1987), and papers quoted therein.
51. Ziółkowski, J., in "Proceedings, 9th European Chemistry of Interfaces Conference, Zakopane, Poland, 1986." *Mater. Sci. Forum* **25/26**, 329 (1988).
52. Ziółkowski, J., *Surf. Sci.* **209**, 536 (1989).
53. Welton-Cook, M. R., and Berndt, W., *J. Phys. C* **15**, 5691 (1982).
54. Benson, G. C., and Claxton T. A., *J. Chem. Phys.* **48**, 1356 (1968).
55. Mackrodt, W. C., Davey, R. J., Black, S. N., and Docherty, R., *J. Cryst. Growth* **80**, 441 (1987).
56. Gorbunova, Yu. E., and Linde, S. A., *Dokl. Akad. Nauk SSSR* **245**, 5864 (1979).
57. Brown, I. D., and Wu, K. K., *Acta Crystallogr. B* **32**, 1957 (1976).
58. Mars, J., and Van Krevelen, D. W., *Chem. Eng. Sci. Suppl.* **3**, 41 (1954).
59. Hodnett, B. K., *Catal. Rev. Sci. Eng.* **27**, 373 (1985) and papers quoted therein.
60. Ai, M., *J. Catal.* **100**, 336 (1986).
61. Buchanan, J. S., and Sundaresan, S., *Appl. Catal.* **26**, 211 (1986).
62. Centi, G., and Trifiro, F., *Chim. Ind.* **68**, 74 (1986).
63. Busca, G., Cavani, F., Centi, G., and Trifiro, F., *J. Catal.* **99**, 400 (1986).
64. Bosch, H., Bruggink, A. A., and Ross, J. R. H., *Appl. Catal.* **31**, 323 (1987).
65. Kruchinin, Yu. A., Mischenko, Yu. A., Nechiporuk, P. P., and Gelbshtein, A. I., *Kinet. Katal.* **25**, 328 (1984).
66. Puttock, S. J., and Rochester, C. H., *J. Chem. Soc. Faraday Trans. 1* **82**, 2773 (1986).